THE CAUSE OF IRIDESCENCE IN RAINBOW ANDRADITE FROM NARA, JAPAN

Thomas Hainschwang and Franck Notari

"Rainbow" andradite from Nara, Japan, occurs as relatively small orangy brown crystals that show attractive iridescence in almost the entire range of the spectrum. The material is nearly pure andradite, as determined by its chemical composition and Vis-NIR and specular reflectance FTIR spectra. Microscopy revealed that two different types of lamellar structures appear to be responsible for the iridescent colors. These lamellar structures cause predominantly thin-film interference and most likely diffraction of light. The terms *interference* and *diffraction* are explained and correlated to the structure and iridescence observed in these garnets.

Garnets with optical phenomena are not commonly encountered, although several types are known, including color-change, star, cat's-eye, and, rarely, iridescent garnets. Color-change garnets are usually pyrope-spessartine, while star garnets are generally almandine or pyrope-almandine. Iridescence in garnet is known only in andradite and grossular-andradite (also called "grandite").

These iridescent garnets are mainly known from Sonora, Mexico (see Koivula, 1987; Koivula and Kammerling, 1988; Badar and Akizuki, 1997; Boehm, 2006). They were initially described several decades ago from a locality in Nevada (Ingerson and Barksdale, 1943); the same authors mentioned similar andradites from Japan (Kamihoki, Yamaguchi Prefecture, Chugoku Region, Honshu Island). Iridescent garnet from Japan's Nara Prefecture (figure 1) was discovered in 2004, and the material has been described by Shimobayashi et al. (2005). More recently, iridescent andradite was found in New Mexico (Burger, 2005). The purpose of this article is to describe the new iridescent garnet from Japan and to attempt a detailed explanation of the color phenomenon observed in this attractive material.

LOCATION, GEOLOGY, MINING, AND PRODUCTION

"Rainbow" andradite from Nara Prefecture was first recovered in early 2004 by several groups of mineral collectors near the old Kouse magnetite mine at Tenkawa in the Yoshino area (Y. Sakon, pers. comm., 2005). This region lies approximately 60 km southeast of Osaka, and is about 400 km east of the Kamihoki locality described by Ingerson and Barksdale (1943; figure 2). Rocks in this area form part of the regional metamorphic Chichibu belt, which lies just south of the Sanbagawa belt (Takeuchi, 1996).

The first garnets recovered were not of high quality, but in September 2004 a local mineral collector (J. Sugimori) found an outcrop containing gem-quality andradite (i.e., strongly iridescent and relatively "clean" material). Over the next four months, he used hand tools to follow the vein to

See end of article for About the Authors and Acknowledgments.
GEMS & GEMOLOGY, Vol. 42, No. 4, pp. 248–258.

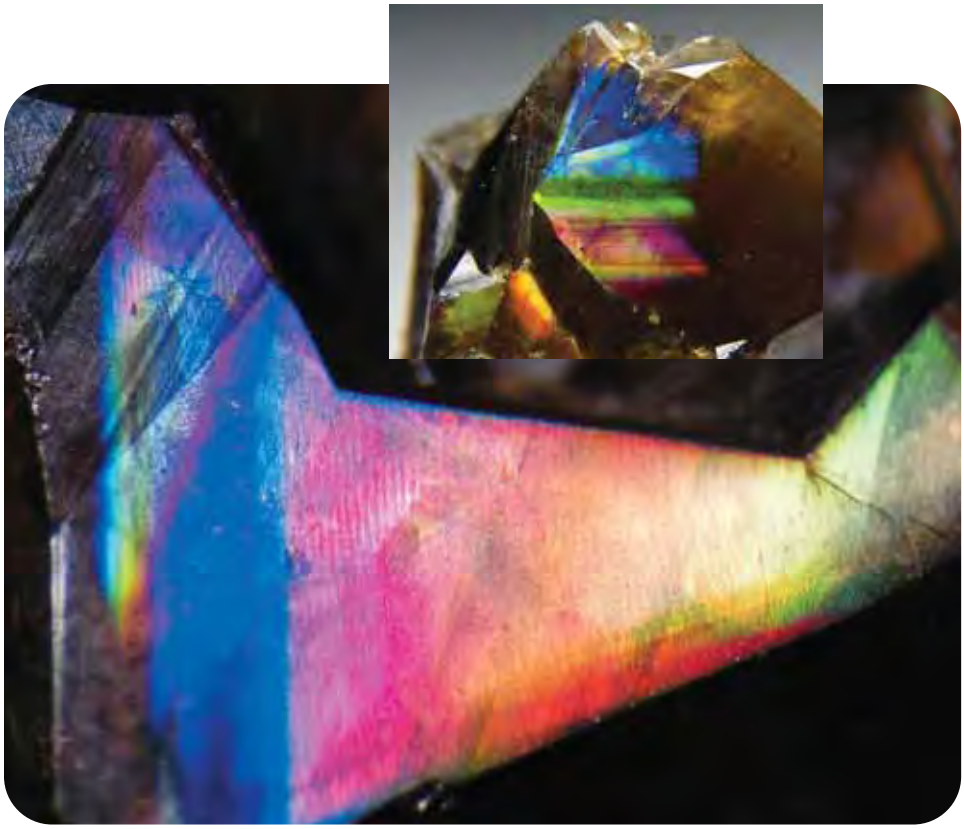

Figure 1. A new source of Rainbow andradite from Nara, Japan, has produced samples with spectacular iridescence, as seen in these unpolished specimens. The crystal face on the left (photomicrograph by T. Hainschwang) is magnified 20×, and the crystal in the inset is 1.7 cm wide (photo by Ms. Bee).

a depth of 5 m. Well-formed crystals showing spectacular iridescence (again, see figure 1) have been sold through the Internet and mineral dealers in Japan. Several hundred kilograms of this Rainbow andradite were recovered, and a small proportion of it was gem quality. Some cabochons have been cut, and rare faceted examples also exist (figure 3). In August 2005, local authorities from Tenkawa village prohibited additional garnet recovery from the area to curtail a mining rush (Y. Sakon, pers. comm., 2005).

MATERIALS AND METHODS

To characterize this material, and better understand the cause of the phenomenon, we examined 60 iridescent garnets from Nara that we obtained from Japanese gem and mineral dealers involved with mining there: a 2.19 ct freeform cabochon (again, see figure 3), three rough samples with polished faces (4.84, 6.12, and 8.03 ct), and 56 rough samples (0.25–3.60 g). For comparison, we examined one partially polished Rainbow garnet of 18.82 ct from Sonora, Mexico.

All samples were examined with a gemological microscope, using reflected and transmitted light, to study their iridescence and microstructure. The luminescence of all the samples was observed using a standard long- and short-wave ultraviolet (UV) lamp (365 and 254 nm, respectively). We determined refractive index and specific gravity (by hydrostatic weighing) for three of the Nara samples.

We used a JEOL 4800 scanning electron microscope (SEM) equipped with an energy-dispersive X-ray (EDX) spectrometer to obtain images in backscattered electron (BSE) mode and semiquantitative chemical point analyses of one 6.22 ct Nara sample. The sample was prepared as a cuboid, with one face polished parallel to a dodecahedral face and four faces polished perpendicular to dodecahedra, in order to resolve the structure of the material; the dodecahedral face remained unpolished. The beam voltage was 15 kV, with a beam current varying from 10 to 200 pA, depending on the magnification used.

The trace-element composition of five larger (8.40–15.87 ct) Nara crystals was investigated with a Thermo Noran QuanX energy-dispersive X-ray fluorescence (EDXRF) system with a Si detector cooled by a Peltier battery. The EDXRF spectra were recorded with acquisition times of 300–1000 seconds, under vacuum to limit the presence of argon, and with sample rotation to avoid diffraction artifacts.

Figure 2. Rainbow andradite from Nara Prefecture was first recovered in early 2004 from the Tenkawa area, located approximately 60 km southeast of Osaka. This deposit is about 400 km east of Japan's original source for this garnet, near Kamihoki.

The infrared spectra of five Nara samples exhibiting smooth crystal faces were recorded at 4 cm^{-1} resolution with a PerkinElmer Spectrum BXII FTIR spectrometer equipped with a Deuterated Tri-Glycine Sulfate (DTGS) detector. A PerkinElmer fixed angle specular reflectance accessory was used for specular reflectance spectra.

We recorded visible–near infrared (Vis-NIR) absorption spectra in the 400–1000 nm range for three highly transparent samples and a small trans-

Figure 3. Both cabochon-cut and faceted Rainbow andradite have been produced, typically in freeform shapes. The cabochon on the left weighs 2.19 ct (photo by T. Hainschwang) and the faceted stones on the right are 6.43–11.39 ct (gift of Keiko Suehiro, GIA Collection nos. 36136–36138; photo by C. D. Mengason).

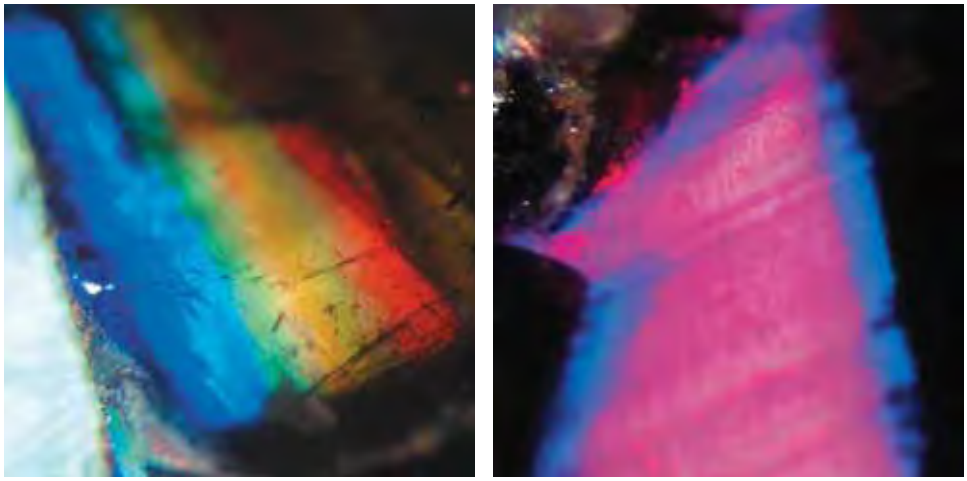

Figure 4. Very colorful and strong iridescence, varying from a range of spectral colors (left) to broad flashes of a single color (right), can be seen in the andradite as the viewing angle changes. Colors such as these were seen on faces oblique to {110}. Photomicrographs by T. Hainschwang; magnified 40× (left) and 60× (right).

parent chip (in order to resolve the 440 nm band), using a custom-made SAS2000 system equipped with an Ocean Optics SD2000 dual-channel spectrometer with a resolution of 1.5 nm. A 2048-element linear silicon CCD detector was employed.

RESULTS

Standard Gemological Testing. All of the Nara garnets had an orangy brown bodycolor, but they exhibited a variety of iridescent colors. Depending on the viewing orientation and the particular crystal face, the phenomenon varied from a single color to a range of colors that shifted as the face was moved (see, e.g., figure 4). Some samples also exhibited "white" flashes that appeared to result from several overlapping colors due to the combined interference from multiple layers.

Microscopic examination indicated the presence of a rather complex lamellar (thin-layered) structure (figure 5). Observation of well-formed dodecahedral crystals demonstrated that the iridescence-causing lamellae were most probably oriented parallel to the dodecahedral {110} faces. Thus, six sets of lamellae were present in these garnets, each parallel to two {110} faces. These lamellae caused broad flashes of one or two nonspectral colors (usually "golden," pinkish red, and blue-green) visible on the {110} faces, always of a relatively weak intensity (figure 6). ("Nonspectral" colors are combinations of spectral colors, which can be seen as a continuous spectral distribution or a combination of primary colors; most colors are nonspectral mixtures.) Brighter and more varied colors were seen on faces oblique to the {110} faces (again, see figures 1 and 4). These irregular striated faces were apparently formed by intergrowth, distortion, and possibly twinning. According to Shimobayashi et al. (2005), the {211} trapezohedral faces are also present on some of the Nara garnets, but we did not see them on our samples. The iridescent colors were not only observed on the surface of the garnets, but they were also seen deep within the more transparent stones.

Besides the lamellar structure parallel to {110}, we also observed an irregular, wavy, step-like

Figure 5. A complex lamellar structure was apparent in the garnets. Thin-film lamellae oriented parallel to the dodecahedral {110} faces formed the predominant microstructure of the bright, colorful parallel bands. Photomicrograph by T. Hainschwang; magnified 10×.

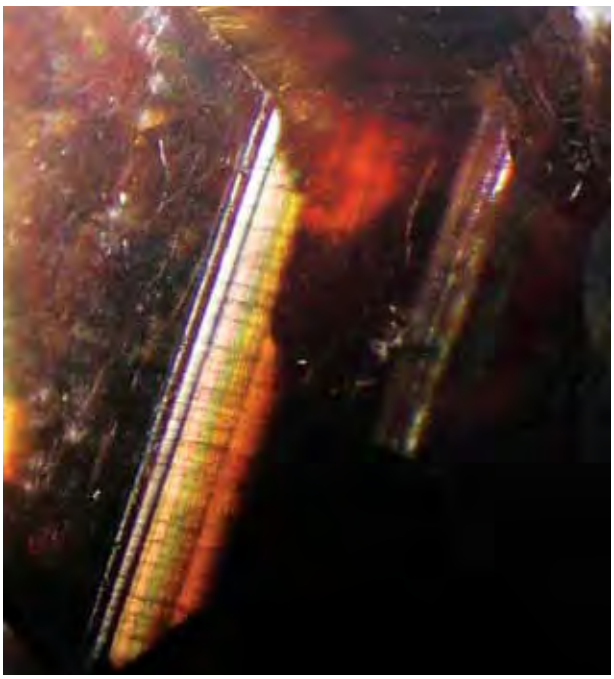

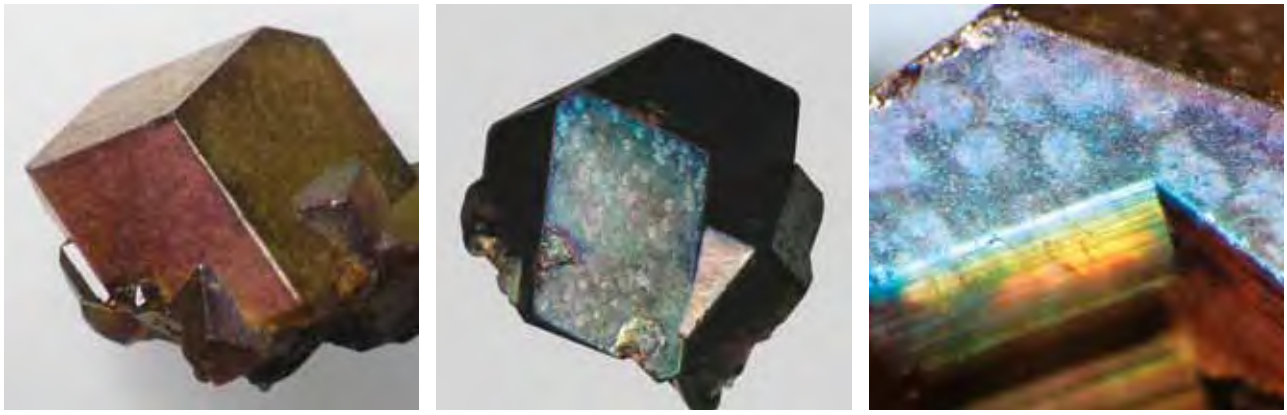

Figure 6. Weak iridescence created broad flashes of nonspectral colors on the dodecahedral {110} faces of the Nara andradites. The colors included "golden" and pinkish red (left, 6.44 ct), greenish blue (center, 9.16 ct), and less commonly bluish purple (right, magnified 15×). The photo on the right also shows (at bottom) the intense lamellar iridescence that is oblique to the dodecahedral face. Photos by T. Hainschwang.

lamellar structure on the dodecahedral faces (figure 7), which was more distinct on practically all faces inclined to the dodecahedra. These two types of lamellar structure are apparently unrelated growth phenomena. Shimobayashi et al. (2005) measured a spacing of ~10–20 μm in the wavy structure; however, they did not assign any phenomenon to these lamellae. In contrast, our microscopic observations suggested that this lamellar structure *does* play a role in the iridescence, even though the lamellae are relatively widely spaced, clearly above the spacing of 100–1000 nm required for a thin-film interference phenomenon (Hirayama et al., 2000). On certain faces, crossed iridescent colors could be seen that appeared to be caused by both the narrow lamellae and the widely spaced wavy lamellae (figure 8). We believe that the moiré-like pattern caused by these crossed iridescent colors is also the result of an interference effect: The crossed grids cause interference and therefore appear distorted.

The refractive index of these garnets was above the limit of the refractometer (>1.81), as expected for andradite. The specific gravity varied slightly from 3.79 to 3.82. As expected for iron-bearing garnets, the samples were inert to short- and long-wave UV radiation.

EDXRF Chemical Analysis. The EDXRF data confirmed that these samples were basically the calcium-iron garnet andradite. Traces of Al and Mn were detected, which most likely indicated very small grossular and spessartine components.

SEM-BSE Imaging and EDX Chemical Analysis. The SEM analysis was performed on a face polished perpendicular to {110}. BSE imaging (figure 9) revealed a structure consisting of fine lamellae (with different chemical compositions) parallel to

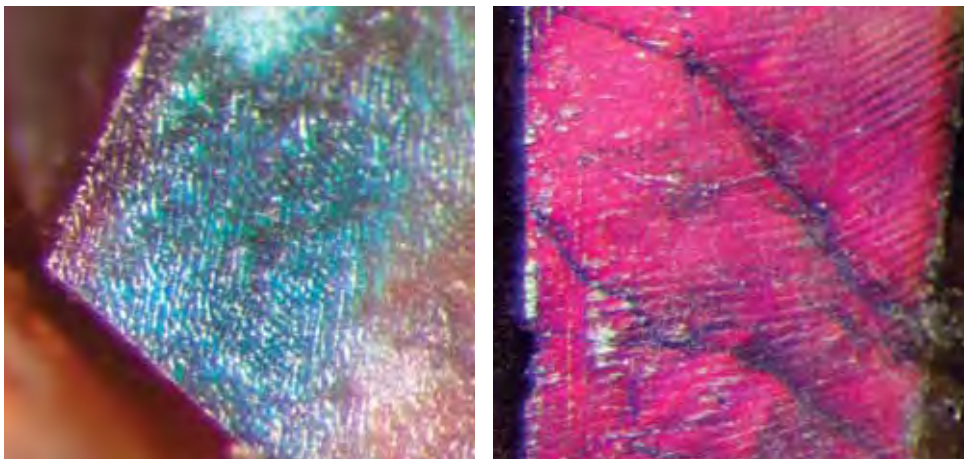

Figure 7. In addition to the fine lamellar structures parallel to {110}, coarser-scale, wavy, step-like structures were seen on practically all faces inclined to the dodecahedra. They appear to produce iridescence colors through a diffraction effect. Photomicrographs by T. Hainschwang; magnified 30× (left) and 45× (right).

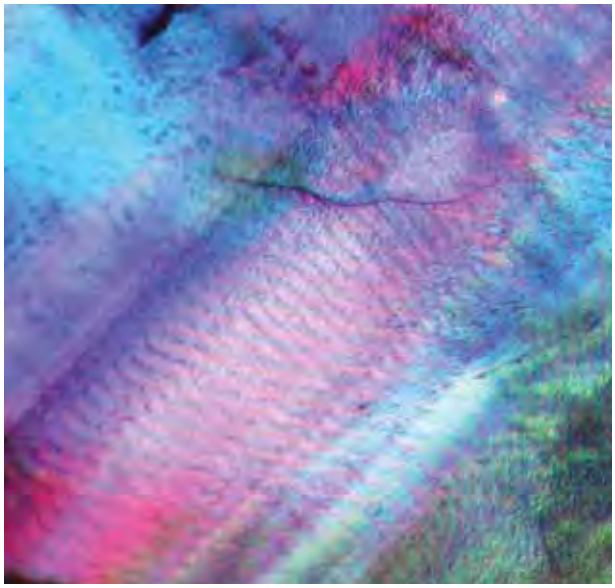

Figure 8. On some of the faces, a moiré pattern was visible, which was apparently related to the wavy structure seen on most of the faces of these garnets. The example shown here has overlapping bright pink to blue to greenish blue iridescence on a face that is oblique to a dodecahedral face. Photomicrograph by T. Hainschwang; magnified 25×.

the {110} face. In the BSE image, darker zones are of lower mean atomic number and lighter zones are of higher mean atomic number.

The lamellae were of varying thicknesses, ranging from about 100 nm to approximately 10 µm; they appeared to average 100–1000 nm (0.1–1 µm). This range is in good agreement with that determined by Shimobayashi et al. (2005).

The semiquantitative EDX chemical point analyses performed on darker and lighter lamellae indicated higher aluminum and lower iron in the darker (lower mean atomic number) zones, whereas the lighter (higher mean atomic number) zones were richer in iron and poorer in aluminum. The darker zones on the BSE image contained about 1–1.5% less iron than the brighter zones and about the same or more aluminum. Thus, the brighter lamellae were nearly pure andradite ($Ca_3Fe_2[SiO_4]_3$), and the darker ones were andradite with a slightly elevated grossular ($Ca_3Al_2[SiO_4]_3$) component.

The minute spessartine component (i.e., manganese) detected by EDXRF analysis was not identified by the SEM-EDX technique, since the concentration was below the detection limit of the instrument.

FTIR Spectroscopy. The specular reflectance FTIR spectra indicated that the samples were almost pure andradite (commonly a perfect match with our reference spectrum; see figure 10).

Vis-NIR Spectroscopy. Vis-NIR spectroscopy (figure 11) showed a typical andradite spectrum, with

Figure 9. In this backscattered electron (BSE) image of the fine lamellae parallel to {110}, the brighter zones (with a higher mean atomic number) correspond to pure andradite, while the darker zones (with a lower mean atomic number) are andradite with a grossular component. BSE image width ~80 µm.

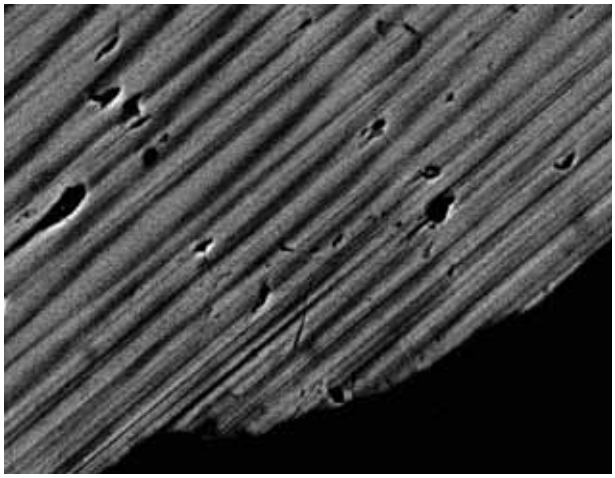

Figure 10. A comparison of the specular reflectance FTIR spectra of the Japanese Rainbow garnet with andradite (demantoid) from Russia and grossular (tsavorite) from Kenya indicates that the Japanese material is almost pure andradite.

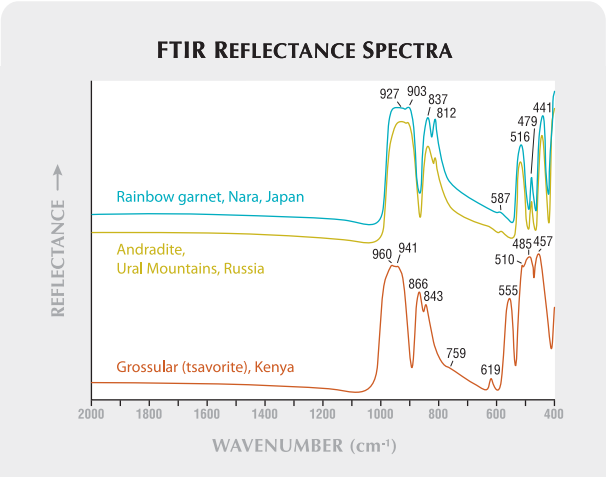

a distinct absorption at 440 nm and a very broad band centered in the near-infrared range at 860 nm, both assigned to Fe^{3+} (Manning, 1967). In thicker specimens, the 440 nm absorption could not be resolved due to complete absorption starting at about 450 nm. In addition, a very weak band at 480 nm was detected.

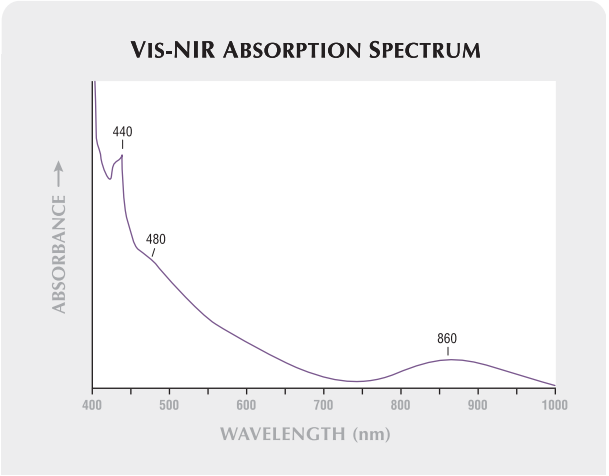

Figure 11. The Vis-NIR spectrum of a small transparent chip of Rainbow andradite is characterized by Fe^{3+}-related absorptions at 440 and 860 nm, plus a weak broad band at 480 nm. The Fe^{3+}-related absorptions are encountered in all andradite.

DISCUSSION

The Nara locality in Japan represents the second discovery of a commercial source for attractive iridescent garnets after Sonora, Mexico. However, the Japanese material appears very different from the Mexican garnets, which have a more greenish bodycolor and show lamellar stripe-like iridescence, sometimes causing a star (figure 12). The Japanese garnets may resemble some brown opals such as those from Ethiopia (e.g., figure 13), and the iridescence is similar to that of high-quality labradorite from Finland.

The iridescence in this Japanese Rainbow andradite is caused by their lamellar structure: alternating microscopic layers of slightly different composition and varying width. Some layers are nearly pure andradite, while the others are andradite with a grossular component. The spacing of the layers, as revealed by SEM-BSE imaging, is suitable for thin-film interference of visible light, and diffraction-related interference may occur when light hits the edges of these layers. (See box A for a more detailed discussion of diffraction and interference, and the distinctions between them.) The chemical differences detected in adjacent layers and the associated differences in R.I., combined with this finely layered structure, clearly point toward multilayer thin-film interference as the main cause of the colorful iridescence.

Both diffraction grating and multilayer interference structures are present when the garnets are viewed at oblique angles to the dodecahedral faces. This explains why the most intense iridescent colors can be observed on faces oblique to {110}. The much weaker and less colorful iridescence visible

Figure 12. Iridescent Mexican "grandite" (grossular-andradite) garnets have a different appearance from the Japanese material. The 18.82 ct Mexican garnet shown on the left has a distinct four-rayed star. Its layer-like iridescence (right, magnified 30×) is quite distinct from that of the Japanese Rainbow andradite. Photos by T. Hainschwang.

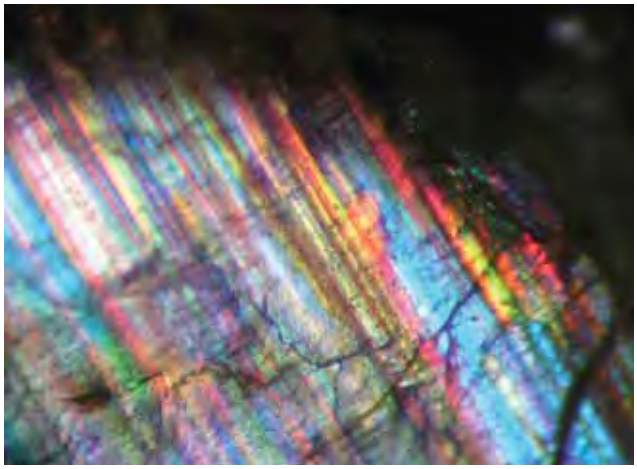

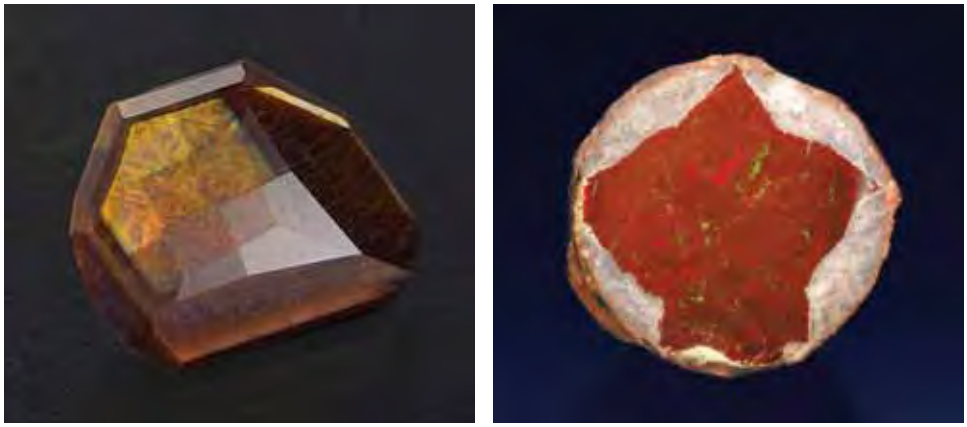

Figure 13. In some cases, the Japanese Rainbow andradite (left) resembles brown opal from Ethiopia (right). The 6.43 ct andradite is a gift of Keiko Suehiro, GIA Collection no. 36137 (photo by C. D. Mengason). The 41.2 g Ethiopian opal nodule is GIA Collection no. 36538 (photo by Robert Weldon).

on {110} faces (figure 6) can be explained by a simple thin-film interference effect.

The other, rather wavy step-like structure visible on almost all faces is likely *not* responsible for any color dispersion due to thin-film interference, because its spacing is much greater than the wavelength of visible light. However, some weaker iridescent colors, which overlap the dominant iridescent colors (figure 7), appear to be caused by a diffraction effect from this structure. This may be explained by comparison to a planar diffraction grating, which will disperse visible light even with a spacing of 20 gratings/mm (a spacing of 50 µm; see, e.g., Newport Corp., 2006). The wavy lamellae, with their step-like surface, could act like a planar diffraction grating having between 50 and 100 gratings/mm. Similar effects can be seen with the low groove density (less than 87 grooves/mm) present in the shells of most mollusks; Liu et al. (1999) related these grooves to weak iridescence caused by diffraction. Indeed the more widely spaced, wavy, step-like lamellar structure in the garnets is very reminiscent of the step-like structure seen in the nacreous aragonite layer of shell (Liu et al., 1999; Fengming et al., 2004).

However, shell iridescence has also been described as a mixed-layer interference and diffraction phenomenon (Tan et al., 2004), and as a thin-film interference phenomenon (Fritsch and Rossman, 1988). A similar structure consisting of both straight lamellae parallel to {110} and wavy lamellae has been described in iridescent garnets from the Adelaide mining district, Nevada, by Akizuki et al. (1984). The same authors described the lack of this wavy structure in iridescent garnets from Kamihoki, Japan.

Further evidence for a combination of fine lamellae and a wavy lamellar (diffraction grating) structure as the cause of iridescence in these garnets is provided by the moiré pattern visible on many of the faces (again, see figure 8). Moiré patterns are caused by interference due to the superposition of two similarly spaced fine patterns, such as grids; interference on these grids results in their distorted appearance, as seen in the two intersecting sets of iridescent color lamellae in figure 8. In these garnets, we have a total of six sets of straight, narrow multilayer structures (each of them following two of the 12 {110} faces) plus the larger, wavy lamellar structure that does not relate to the dodecahedral faces. Thus, on faces oblique to a simple {110} face, several of these structures and their associated color patterns will overlap and cause very colorful iridescence.

Combinations of multilayer interference and lamellar diffraction grating structures have been credited with causing the bright blue iridescence seen in *Morpho didius* butterflies (Vukusic et al., 1999; Iwase et al., 2004) and, together with scattering, for the bright green iridescence in *Papilio blumei* butterflies (Tada et al., 1999). In *Morpho didius* butterflies, the iridescence-causing structure consists of overlapping tiles on which Christmas tree–like microstructures can be seen; these structures cause multilayer interference in one direction, and diffraction in an orientation approximately perpendicular to the layer-like structure due to its "roughness."

CONCLUSIONS

First discovered at this locality in 2004, andradite from Nara, Japan, shows an attractive iridescence that is probably caused by a combination of a narrowly spaced lamellar structure following the rhombic dodecahedron {110} and another wavy, widely spaced, step-like lamellar structure (not parallel to the {110} faces) that is visible on almost

BOX A: IRIDESCENCE, INTERFERENCE, AND DIFFRACTION

Traditionally, the term *iridescence* has been used in gemology to describe only thin-film interference in specific phenomenal gems, such as iris agate, Ammolite, and pearls (see e.g., Fritsch and Rossman, 1988). Today, *iridescence* is frequently used to describe *any* diffraction and/or thin-film interference–related color phenomena. This is likely because interference and diffraction in minerals are closely related phenomena that often occur together, and it can be very difficult to distinguish them without a detailed analysis of the near-surface structure (Vukusic et al., 1999; Iwase et al., 2004).

The main difference between diffraction and thin-film interference is the interference-causing path of the light rays. In diffraction, light waves pass through a grating—or, in the case of garnet, reflect from a patterned, edged surface—and interact with one another. The spacing of these edges needs to be regular and narrow, but not necessarily on the order of the wavelength of visible light; in diffraction gratings, a spacing as low as 20 grooves/mm is sometimes used to create diffraction-related interference and thus disperse the white light into its spectral colors (Newport Corp., 2006). In multilayer films, both reflected and refracted light waves from each boundary between the layers interact with one another, and the interference may be observed if the film thickness is within the range of visible light (Hirayama et al., 2000). Some details on the two mechanisms are summarized below; an in-depth discussion of the theory, mathematics, and physics of diffraction and interference can be found, for example, in Born and Wolf (1999).

The effects caused by the coherent addition of wave amplitudes are known as "interference effects" (Born and Wolf, 1999). When two (or more) waves with equal amplitudes are **in phase** (i.e., crest meets crest and trough meets trough), then the waves enhance each other, and the resulting wave is the sum of their amplitudes; this is called *constructive interference*. If the waves are **out of phase** (i.e., crest meets trough), then the waves cancel each other out completely; this is *destructive interference* (see, e.g., Mathieu et al., 1991).

Thin-film interference of visible light occurs when light interacts with a lamellar material consisting of fine layers that have different refractive indices. These layers can be of any state: gaseous, liquid, solid, or even "empty" (vacuum). For example, a soap bubble shows iridescence due to the thin-film interference between the outside-air/soap and soap/inside-air interfaces. The width of the layers must be approximately the same as the wavelength of light, that is, somewhere between 0.1 and 1 µm. When light passes through such a material, it is refracted, and then parts of it are reflected off each layer. The reflected waves are partially or completely in phase or out of phase, thus creating constructive or destructive interference. An example of simple double-layer interference of a "white" light source is shown in figure A-1. The figure has been simplified because the interference of "white" light is quite complicated, since it is composed of all wavelengths from the UV to the NIR, and each wavelength is refracted differently when entering (and at every boundary with) a thin film.

Diffraction is caused by the bending, spreading, and subsequent overlapping of a wavefront when passing through a tiny opening or openings in an otherwise opaque obstacle (e.g., the slits in a diffraction grating) or at boundaries and edges (figure A-2). The light passing through the opening(s) or reflecting off a patterned, edged surface may experience destructive and constructive interference, thus creating dark and bright fringes, respectively, when the openings or edges of the lamellae are small enough (see, e.g., Mathieu et al., 1991). The slit width or pattern spacing needs to be small but not necessarily on the order of the wavelength of light (see, e.g., Liu et al., 1999; Newport Corp., 2006). Experiments performed by one of the authors (TH) with translucent curtain fabric with thread thickness ±0.08 mm (80,000 nm) and spacing of 0.25 mm (250,000 nm) between both the horizontal and vertical threads confirm that such a relatively large grid will cause a very distinct diffraction pattern and light dispersion. With a diffraction grating, the effect functions as follows: A large number of identical, equally spaced slits (hence the occasional use of the term *multiple-slit interference*) or lamellae edges will cause many positions of entirely destructive interference fringes between intense constructive interference fringes. A planar diffraction grating used for visible light has a groove density of about 20 to 1800 grooves per mm. A number of different theories exist to explain diffraction; for more details see Born and Wolf (1999).

It is important to note that these effects are not limited to visible light. *Bragg diffraction*, also called *Bragg interference*, is the term for the scattering and interference effect that occurs when X-rays interact with a crystal lattice.

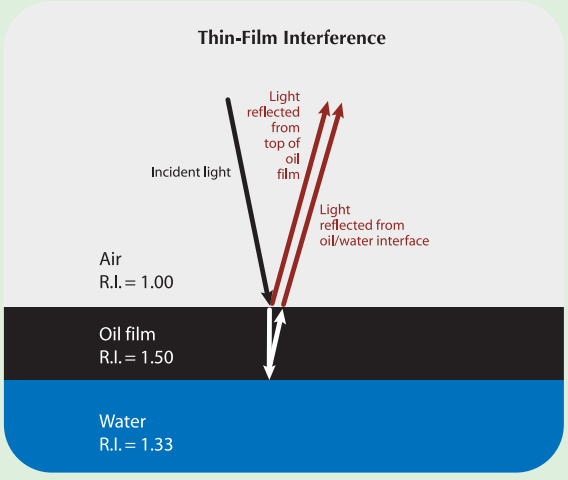

Figure A-1. This diagram shows thin-film interference of monochromatic light from a simple double-film consisting of a layer of oil floating on water.

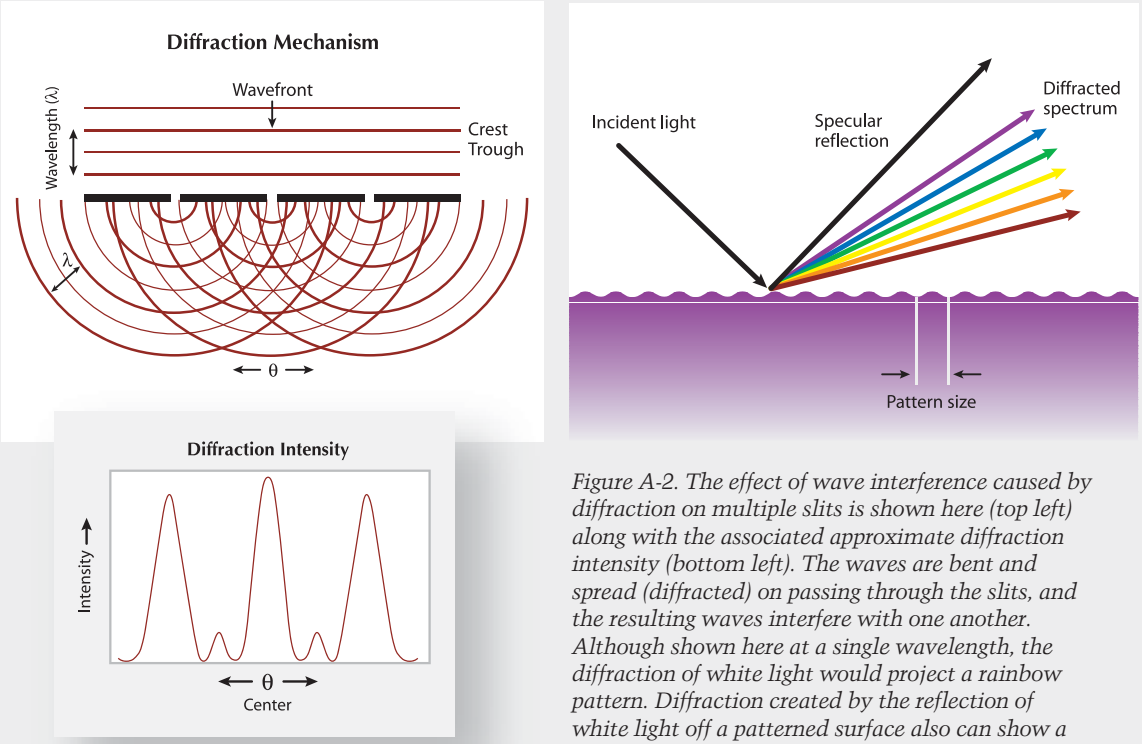

Figure A-2. The effect of wave interference caused by diffraction on multiple slits is shown here (top left) along with the associated approximate diffraction intensity (bottom left). The waves are bent and spread (diffracted) on passing through the slits, and the resulting waves interfere with one another. Although shown here at a single wavelength, the diffraction of white light would project a rainbow pattern. Diffraction created by the reflection of white light off a patterned surface also can show a rainbow pattern (top right).

German physicist Max von Laue suggested in 1912 that molecules in crystalline substances could be used as diffraction gratings. He found that X-rays were reflected and scattered from the individual atoms distributed in equally spaced lattice planes and that the reflected and scattered waves would constructively and destructively interfere to create X-ray diffraction patterns (see, e.g., Diehl and Herres, 2004). Based on Laue's findings, English physicists W. H. Bragg and his son W. L. Bragg explained why the cleavage faces of crystals appear to reflect X-ray beams at certain angles of incidence. The Bragg equation describes at what angles X-rays will be most efficiently diffracted by a crystal when the X-ray wavelength and atomic distance are known (Diehl and Herres, 2004).

Both Bragg's law and diffraction can be used to explain play-of-color in opal, where light beams are diffracted from opposite sides of very small, regularly arranged spheres with diameters of 150–400 nm (Fritsch and Rossman, 1988; Townsend, 2001). Bragg's law can also be applied to the theory of diffraction gratings. The atoms of a crystalline substance and the spheres in opal are very often represented as *layers* to explain the Bragg law of diffraction, since they are equally and regularly spaced. Such diagrams are unfortunately confusing, since they often appear identical to figures explaining thin-film interference phenomena. Again, it must be emphasized that diffraction does not take place on the layers themselves, but rather on individual atoms or spheres.

In gem materials, "pure" diffraction-related interference of light likely is limited to opals showing play-of-color, since the opal structure behaves much like a crystalline structure consisting of tiny atoms: The size of the atoms (approximately equal to X-ray wavelengths) allows diffraction of X-rays, while the size of the opal spheres (approximately equal to the wavelength of visible light) allows diffraction of visible light.

The effect of a multilayer substance such as "spectrolite" feldspar (labradorite) on light has been described as a diffraction effect by certain authors (e.g., Fritsch and Rossman, 1988) and these authors also limited the term *thin-film interference* to a simple double-film (as in iris quartz) such as shown in figure A-1. In the opinion of the present authors, double-layer and multilayer effects both represent thin-film interference phenomena, with the multilayers being more complex than the simple double-layers (see Hirayama et al., 2000).

Therefore, we conclude that the phenomenon of iridescence in gem materials is always an interference phenomenon; the only difference is whether the interference is caused by thin-film interference or by diffraction. Thus, there are gems with iridescence caused purely by thin-film interference (e.g., iris quartz); others with diffraction-related interference (e.g., diffraction of visible light in opal); and still others where dominant thin-film interference combined with some diffraction occurs, as in the Japanese Rainbow andradite described in this article.

all faces. The iridescence on the {110} faces likely is caused by thin-film interference from the straight lamellae, which have a separation of 100–1000 nm. The wavy lamellae, with a spacing of 40 μm, cannot produce iridescence by thin-film interference, and therefore possibly act similar to a diffraction grating. The combination of these two optical effects creates the striking iridescence observed in this Rainbow andradite, which can rival the phenomenal colors of the finest "spectrolite" feldspar (labradorite) from Finland. In some cases, these stones may resemble brown opals from Ethiopia. Due to the prohibition of further garnet recovery by the local authorities from Tenkawa village, the material is slowly becoming scarce in the market but samples can still be seen, especially on the Internet. Future availability of this attractive garnet will thus solely depend on the local authorities in Japan.

ABOUT THE AUTHORS
At the time this article was prepared, Mr. Hainschwang (thainschwang@yahoo.com) was research gemologist, and Mr. Notari was research manager, at GIA GemTechLab in Geneva, Switzerland.

ACKNOWLEDGMENTS: The authors are grateful to Dr. Emmanuel Fritsch (Institut des Matériaux Jean Rouxel, Nantes, France) for SEM analysis and fruitful discussions, and to Yuichi Sakon (Hokkaido, Japan) for supplying photos and information on the mining and geology of the garnet deposit.

REFERENCES

Akizuki M., Nakai H., Suzuki T. (1984) Origin of iridescence in grandite garnet. *American Mineralogist*, Vol. 69, pp. 896–901.

Bader M.A., Akizuki M. (1997) Iridescent andradite garnet from the Sierra Madre Mountains, Sonora, Mexico. *Neues Jahrbuch für Mineralogie, Monatshefte*, Vol. 12, pp. 529–539.

Boehm E. (2006) Gem News International: Update on iridescent andradite from Mexico. *Gems & Gemology*, Vol. 42, No. 2, pp. 170–171.

Born M., Wolf E. (1999) *Principles of Optics: Electromagnetic Theory of Propagation, Interference and Diffraction of Light*, 7th ed. Cambridge University Press, Cambridge, UK, 952 pp.

Burger F. (2005) Gems in the parking lot. *Lapidary Journal*, Vol. 59, No. 2, pp. 80–82.

Diehl R., Herres N. (2004) X-ray fingerprinting routine for cut diamonds. *Gems & Gemology*, Vol. 40, No. 1, pp. 40–57.

Fengming H., Zonghui C., Hua T., Ying Z., Ziqi Z., Mingxing Y. (2004) The microstructure of the shell and cultured blister pearls of *Pteira penguin* from Sanya, Hainan, China. *Journal of Gemmology*, Vol. 29, No. 1, pp. 37–47.

Fritsch E., Rossman G.R. (1988) An update on color in gems. Part 3: Colors caused by band gaps and physical phenomena. *Gems & Gemology*, Vol. 24, No. 2, pp. 81–102.

Hirayama H., Kaneda K., Yamashita H., Monden Y. (2000) An accurate illumination model for objects coated with multilayer films. In A. de Sousa and J. Torres, Eds., *Eurographics 2000 Short Presentations*, Interlaken, Switzerland, August 20–25, pp. 145–150.

Ingerson E., Barksdale J.D. (1943) Iridescent garnet from the Adelaide mining district, Nevada. *American Mineralogist*, Vol. 28, No. 5, pp. 303–312.

Iwase E., Matsumoto K., Shimoyama I. (2004) The structural-color based on the mechanism of butterfly wing coloring for wide viewing angle reflective display. 17th IEEE International Conference on Micro Electro Mechanical Systems (MEMS '04), Maastricht, The Netherlands, Jan. 25–29, www.leopard.t.u-tokyo.ac.jp/PDF/iwase3.pdf [date accessed: 01/05/06].

Koivula J.I., Ed. (1987) Gem News: Iridescent andradite garnets. *Gems & Gemology*, Vol. 23, No. 3, pp. 173–174.

Koivula J.I., Kammerling R.C., Eds. (1988) Gem News: More on Mexican andradite. *Gems & Gemology*, Vol. 24, No. 3, pp. 120–121.

Liu Y., Shigley J.E., Hurwit K.N. (1999) Iridescent color of a shell of the mollusk *Pinctada margaritifera* caused by diffraction. *Optics Express*, Vol. 4, No. 5, pp. 177–182.

Manning P.G. (1967) The optical absorption spectra of some andradite and the identification of the $^6A_1 \rightarrow {}^4A_1\ {}^4E(G)$ transition in octahedrally bonded Fe^{3+}. *Canadian Journal of Earth Sciences*, Vol. 4, pp. 1039–1047.

Mathieu J.P., Kastler A., Fleury P. (1991) *Dictionnaire de Physique*, 3rd ed. Masson et Eyrolles, Paris.

Newport Corp. (2006) Diffraction gratings. www.newport.com/Diffraction%20Gratings/1/productmain.aspx [date accessed: 12/12/05].

Shimobayashi N., Miyake A., Seto Y. (2005) Rainbow garnet from Tenkawa village in Nara. *Gemmology*, Vol. 36, No. 435, pp. 4–7 [in Japanese with English insert].

Tada H., Mann S.E., Miaoulis I.N., Wong P.Y. (1999) Effects of a butterfly scale microstructure on the iridescent color observed at different angles. *Optics Express*, Vol. 5, No. 4, pp. 87–92.

Takeuchi M. (1996) Geology of the Sanbagawa, Chichibu and Shimanto belts in the Kii Peninsula; Yoshino area in Nara Prefecture and Kushidagawa area in Mie Prefecture. *Chishitsu Chosajo Geppo*, Vol. 47, No. 4, pp. 223–244 [in Japanese].

Tan T.L., Wong D., Lee P. (2004) Iridescence of a shell of mollusk *Haliotis glabra*. *Optics Express*, Vol. 12, No. 20, pp. 4847–4854.

Townsend I. J. (2001) The geology of Australian opal deposits. *Australian Gemmologist*, Vol. 21, pp. 34–37.

Vukusic P., Sambles J.R., Lawrence C.R., Wootton R.J. (1999) Quantified interference and diffraction in single *Morpho* butterfly scales. *Proceedings of the Royal Society B*, Vol. 266, pp. 1403–1411.

Spring 1999
The Identification of Zachery-Treated Turquoise
Russian Hydrothermal Synthetic Rubies and Sapphires
The Separation of Natural from Synthetic Colorless Sapphire

Summer 1999
On the Identification of Emerald Filling Substances
Sapphire and Garnet from Kalalani, Tanzania
Russian Synthetic Ametrine

Fall 1999—Special Issue
Special Symposium Proceedings Issue, including:
Observations on GE-Processed Diamonds, Abstracts of Featured Speakers, Panel Sessions, War Rooms, and Poster Sessions

Winter 1999
Classifying Emerald Clarity Enhancement at the GIA Gem Trade Laboratory
Clues to the Process Used by General Electric to Enhance the GE POL Diamonds
Diopside Needles as Inclusions in Demantoid Garnet from Russia
Garnets from Madagascar with a Color Change of Blue-Green to Purple

Spring 2000
Burmese Jade
Lapis Lazuli from Chile
Spectroscopic Evidence of GE POL Diamonds
Chromium-Bearing Taaffeites

Summer 2000
Characteristics of Nuclei in Chinese Freshwater Cultured Pearls
Afghan Ruby and Sapphire
Yellow to Green HPHT-Treated Diamonds
New Lasering Technique for Diamond
New Oved Filling Material for Diamonds

Fall 2000
GE POL Diamonds: Before and After
Sapphires from Northern Madagascar
Pre-Columbian Gems from Antigua
Gem-Quality Haüyne from Germany

Winter 2000—Special Issue
Gem Localities of the 1990s
Enhancement and Detection in the 1990s
Synthetics in the 1990s
Technological Developments in the 1990s
Jewelry of the 1990s

Spring 2001
Ammolite from Southern Alberta, Canada
Discovery and Mining of the Argyle Diamond Deposit, Australia
Hydrothermal Synthetic Red Beryl

Summer 2001
The Current Status of Chinese Freshwater Cultured Pearls
Characteristics of Natural-Color and Heat-Treated "Golden" South Sea Cultured Pearls
A New Method for Imitating Asterism

Fall 2001
Modeling the Appearance of the Round Brilliant Cut Diamond: Fire
Pyrope from the Dora Maira Massif, Italy
Jeremejevite: A Gemological Update

Winter 2001
An Update on "Paraíba" Tourmaline from Brazil
Spessartine Garnet from San Diego County, California
Pink to Pinkish Orange Malaya Garnets from Bekily, Madagascar
"Voices of the Earth": Transcending the Traditional in Lapidary Arts

Spring 2002—Special Issue
The Ultimate Gemologist: Richard T. Liddicoat
Portable Instruments and Tips on Practical Gemology in the Field
Liddicoatite Tourmaline from Madagascar
Star of the South: A Historic 128 ct Diamond

Summer 2002
Characterization and Grading of Natural-Color Pink Diamonds
New Chromium- and Vanadium-Bearing Garnets from Tranoroa, Madagascar
Update on the Identification of Treated "Golden" South Sea Cultured Pearls

Fall 2002
Diamonds in Canada
"Diffusion Ruby" Proves to Be Synthetic Ruby Overgrowth on Natural Corundum

Winter 2002
Chart of Commercially Available Gem Treatments
Gemesis Laboratory-Created Diamonds
Legal Protection for Proprietary Diamond Cuts
Rhodizite-Londonite from the Antsongombato Pegmatite, Central Madagascar

Spring 2003
Photomicrography for Gemologists
Poudretteite: A Rare Gem from Mogok
Grandidierite from Sri Lanka

Summer 2003
Beryllium Diffusion of Ruby and Sapphire
Seven Rare Gem Diamonds

Fall 2003
G. Robert Crowningshield: A Legendary Gemologist
Cause of Color in Black Diamonds from Siberia
Obtaining U.S. Copyright Registration for the Elara Diamond

Winter 2003
Gem-Quality CVD Synthetic Diamonds
Pezzottaite from Madagascar: A New Gem
Red Beryl from Utah: Review and Update

Spring 2004
Identification of CVD-Grown Synthetic Diamonds
Cultured Pearls from Gulf of California, Mexico
X-Ray Fingerprinting Routine for Cut Diamonds

Summer 2004
Gem Treatment Disclosure and U.S. Law
Lab-Grown Colored Diamonds from Chatham
The 3543 cm^{-1} Band in Amethyst Identification

Fall 2004
Grading Cut Quality of Round Brilliant Diamonds
Amethyst from Four Peaks, Arizona

Winter 2004
Creation of a Suite of Peridot Jewelry: From the Himalayas to Fifth Avenue
An Updated Chart on HPHT-Grown Synthetic Diamonds
A New Method for Detecting Beryllium Diffusion–Treated Sapphires (LIBS)

Spring 2005
Treated-Color Pink-to-Red Diamonds from Lucent Diamonds Inc.
A Gemological Study of a Collection of Chameleon Diamonds
Coated Pink Diamond: A Cautionary Tale

Summer 2005
Characterization and Grading of Natural-Color Yellow Diamonds
Emeralds from the Kafubu Area, Zambia
Mt. Mica: A Renaissance in Maine's Gem Tourmaline Production

Fall 2005
A Review of the Political and Economic Forces Shaping Today's Diamond Industry
Experimental CVD Synthetic Diamonds from LIMHP-CNRS, France
Inclusions in Transparent Gem Rhodonite from Broken Hill, New South Wales, Australia

Winter 2005
A Gemological Pioneer: Dr. Edward J. Gübelin
Characterization of the New Malossi Hydrothermal Synthetic Emerald

70 PLUS Years of

GEMS & GEMOLOGY

The Quarterly Journal That Lasts A Lifetime

Order Your BACK ISSUES Today!

	U.S.	Canada	International
Single Issues	$12 ea.	$15 ea.	$18 ea.
Complete Volumes* 1991–2005	$40 ea.	$48 ea.	$60 ea.
Three-year set	$115 ea.	$135 ea.	$170 ea.
Five-year set	$190 ea.	$220 ea.	$280 ea.

*10% discount for GIA Alumni and active GIA students.

Some issues from 1981–1998 are also available. Please call or visit our website for details on these and the 2006 issues as they are published.

Limited Quantities Available.

E-Mail: gandg@gia.edu or visit www.gia.edu
Call Toll Free 800-421-7250 ext. 7142
or 760-603-4000 ext. 7142
Fax: 760-603-4595 or Write: G&G Subscriptions, P.O. Box 9022, Carlsbad, CA 92018-9022 USA